Applied Physics Letters

RESEARCH ARTICLE | AUGUST 13 2018

Direct-to-indirect electronic state transition in dynamically compressed GaAs quantum wells

P. Grivickas; J. F. Geisz; Y. M. Gupta

Appl. Phys. Lett. 113, 072101 (2018)
https://doi.org/10.1063/1.5038723
CHORUS

AIP Publishing

Direct-to-indirect electronic state transition in dynamically compressed GaAs quantum wells

P. Grivickas,[1,a)] J. F. Geisz,[2] and Y. M. Gupta[1]
[1]*Institute for Shock Physics and Department of Physics, Washington State University, Pullman, Washington 99164, USA*
[2]*National Renewable Energy Laboratory, 1617 Cole Blvd., Golden, Colorado 80401, USA*

(Received 4 May 2018; accepted 17 July 2018; published online 13 August 2018)

Dynamic compression of GaAs quantum wells was achieved to examine the direct-to-indirect transition in a reduced dimension semiconductor structure under uniaxial strain conditions. Our results show that the transformation deviates significantly from the electronic structure predictions using bulk deformation potentials. This finding is attributed to the suppression of real-space type-II transitions by quantum state interactions due to the presence of large anisotropic strains. *Published by AIP Publishing*. https://doi.org/10.1063/1.5038723

A key prerequisite for using semiconductors in optoelectronic applications is to ensure that they display a direct bandgap while being strained. Strains can invert the direct bandgap of semiconductors because of the disproportional energy shifts between the direct and indirect conduction bands. In bulk materials, the direct-to-indirect transition (DIT) has been studied primarily using hydrostatic pressure[1] and accounted for by using deformation potentials (DPs) in electronic structure calculations.[2] However, the actual manifestation of such DIT in currently used devices remains minimal due to the limited $<1\%$ lattice mismatch strains obtained at planar heterointerfaces. This situation is expected to change profoundly in future devices utilizing reduced dimension structures. Strains approaching 10% or more are anticipated in semiconductor nanostructures such as nanowires[3] and self-assembled[4] or embedded[5] quantum dots.

Understanding strain induced DIT in nanostructures presents a significant scientific challenge due to the interplay between strain effects and quantum effects, leading to phenomena such as lowering of the DIT threshold values,[6–8] switching to real-space type-II transitions,[6,7,9] the presence of coupling effects,[7,10] or screening by piezoelectric fields.[11] It has been suggested that a detailed description of these phenomena is possible only through atomistic theories.[12] The other important, but less emphasized, factor is the strong anisotropic character of strain fields in nanostructures. In bulk crystals, anisotropic strains lift the degeneracy of electronic states and introduce major changes to their shifts as described by the shear DPs.[2] It was shown, for example, that the usual DIT in GaAs between Γ and X states can be converted into one between Γ and L states when uniaxial strain is applied along the [111] orientation.[13] Accurate prediction of the DIT in nanostructures using shear DPs as semi-empirical, linear-response quantities remains an open question.[14]

Examining the effects of large anisotropic strains in as-grown nanostructures is difficult due to many material quality related issues including strain homogeneity, composition variation, surface passivation, and reproducibility.[8] In principle, these problems can be circumvented by subjecting nanostructures to well-defined external strains, but the two main compression methods used in semiconductor research, hydrostatic pressure and uniaxial stress, do not result in large anisotropic strains relevant to the nanoscale. The former produces large volumetric compression only, while the latter is restricted by material fracture.[15]

Here, we show how dynamic compression can be used to examine large anisotropic strains in reduced dimension structures and apply this approach to examine the DIT phenomenon. As a first demonstration, we chose GaAs quantum wells (QWs) as a prototype quantum structure whose optical properties have been investigated extensively using both hydrostatic pressure[16–19] and uniaxial stress.[20–23] We find that even for the simple case of uniaxial strain compression along the [100] crystallographic orientation, the DIT observed in QWs shows remarkable deviations from the electronic structure predictions using bulk DPs.

Plane compression waves were generated using impact experiments where a moving projectile impacts a stationary target and creates a longitudinal stress σ_{LS} along the wave propagation direction. Due to inertial confinement, a macroscopically exact state of uniaxial strain is produced in the sample. The magnitude and the temporal history of the longitudinal stress in the sample depend on the projectile velocity and the planer discs encapsulating the sample. In the current work, samples were placed between transparent Z-cut quartz or fused silica windows suitable for optical measurements. A schematic representation of the dynamic compression experiments and photoluminescence (PL) measurements in the sample is shown in the inset of Fig. 1. Further details about the dynamic compression experiments, including PL measurements, can be seen in previous studies on bulk semiconductors.[24–26]

The samples investigated consisted of six single GaAs QWs of various thicknesses separated by 100 nm $Al_{0.3}Ga_{0.7}As$ barriers. The structures were grown by atmospheric-pressure organometallic vapor phase epitaxy on a singular (001) GaAs substrate at 700 °C. The thinnest QWs were placed closest to the probed surface to prevent reabsorption effects. The thickness of

[a)]Current address: Lawrence Livermore National Laboratory, Livermore, California 94550, USA

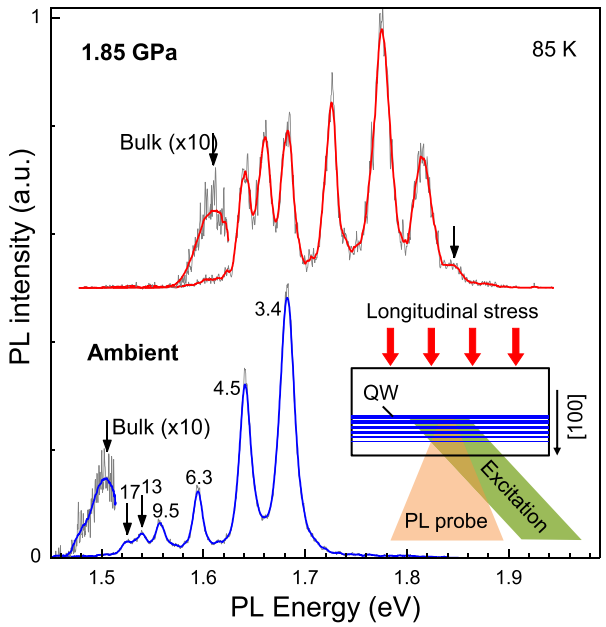

FIG. 1. PL spectra of the QW sample under ambient conditions (bottom) and under shock compression to 1.85 GPa (top). The inset shows the main elements of the dynamic compression experiments.

GaAs QWs ranged from 3.4 to 17 nm as determined from photoluminescence (PL) measurements. Individual samples were cut from the same well-characterized wafer for each dynamic compression experiment. The 1:20 ratio between the sample thickness and lateral dimensions was maintained to ensure uniaxial strain compression for the times of interest.[24–26] The wave propagation direction was chosen to be along the [100] crystallographic orientation of GaAs aligned with the quantization axis of QWs.

Optical emission from QWs was excited using a 532 nm laser and probed using time- and spectrally-resolved PL measurements. Using liquid nitrogen, the whole target was cooled to 85 K to enhance the intensity and spectral resolution of the detected PL peaks. The bottom of Fig. 1 shows the ambient PL spectrum of the QWs. The exact thickness of the QWs (in nm), as labeled in Fig. 1, was determined by comparing the position of the six well-resolved PL peaks to the established free exciton energies in GaAs QWs.[27] The weak PL signal from the GaAs substrate was also detected and used as a reference for comparison with previous dynamic compression experiments on bulk GaAs.[13]

Compression wave profiles reaching the sample were measured using a velocity interferometer system.[28,29] Two types of compression wave profiles, a shock wave and a ramp wave, were produced in the experiments. In both cases, identical conditions of uniaxial strain were created with the sole difference being the temporal history of the longitudinal stress. In the shock wave, a step jump followed by a relatively long state (>100 ns) of constant σ_{LS} provided the best signal-to-noise ratio in our optical measurements. This profile was used to detect a well-defined reference point at 1.85 GPa. In the ramp wave, stress profiles with monotonically increasing σ_{LS} values were generated over a similar time duration, resulting in a gradual compression of the sample stresses up to 5 GPa in a single event experiment. This profile was used to detect the continuous shift of PL peaks with increasing σ_{LS}.

The PL spectrum from the sample shock compressed to 1.85 GPa is shown at the top of Fig. 1. All QW peaks were well resolved in the spectrum and showed a simultaneous shift to higher energies reminiscent of the observations in the bulk GaAs substrate. The shift of the different peaks is shown by the red diamond symbols in Fig. 2(a). The peak shifts under ramp compression are also shown in the same figure (blue circle symbols) together with the previously reported data from the bulk GaAs (open circle symbols).[13] Good agreement between the shock and the ramp data was obtained.

To elucidate the origin of the observed shifts, the electronic structure of GaAs QWs is shown schematically in Fig. 2(b). Different energies of the Γ bands in GaAs and $Al_{0.3}Ga_{0.7}As$ result in the potential wells shown by the solid lines. Free carriers placed in these potentials end up in the quantum states whose separation energies depend on the well widths and on the effective mass of the carriers in the particular band. In the Γ_C conduction band, the single ground state (C) for electrons is formed. In the Γ_V valence band, two distinct ground states emerge for heavy-holes (HHs) and light-holes (LHs). The heavier HH state is higher in energy, leading to primarily C-HH optical transitions at ambient conditions. The transition energy in the PL spectrum is additionally lowered by the exciton binding energies.

The shift of Γ_C and Γ_V bands in compressed GaAs can be reproduced using the volumetric and the shear DPs of GaAs.[30] The corresponding fit using these parameters for the bulk GaAs under uniaxial strain (open symbols) is shown in Fig. 2(a) by the solid curve. The same parameters were used to model the shift of the quantum states, resulting in the dashed and solid curves in Fig. 2(a) for the C-HH and C-LH transitions, respectively. The C-HH transitions were initiated at the ambient positions of the PL peaks, while the C-LH transitions were shifted according to the HH-LH splitting[27] reported in the literature. The calculated shifts match the experimental data well, and the observed slope changes at $\sigma_{LS} < 2$ GPa are attributed to the HH-LH crossover. Such a crossover is best seen in the narrowest or 3.4 nm QW as indicated by the arrow. The clear HH-LH crossover in GaAs

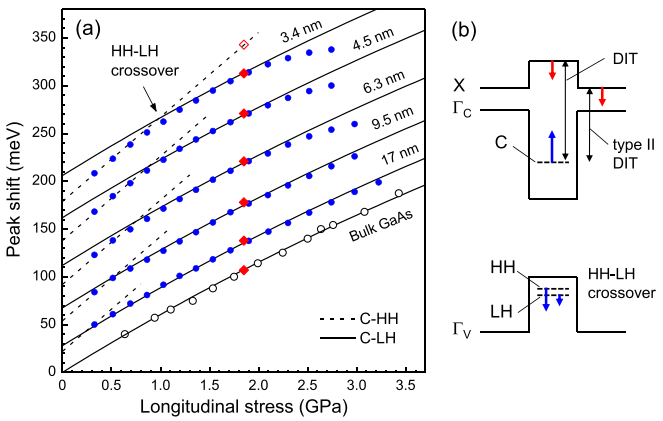

FIG. 2. Shift of the PL peaks in QWs (full symbols) and bulk GaAs (open symbols) due to applied longitudinal stress, σ_{LS}. Red and blue symbols in QWs represent shock and ramp compression data, respectively. The lines show calculated shifts using DPs for bulk GaAs. The right-side of the figure shows a schematic view of the electronic structure of GaAs QWs. The arrows indicate shifts of different states under applied σ_{LS}.

QWs has not been previously resolved due to the limitations in uniaxial stress experiments above 0.5 GPa.[23] The calculations shown also reveal the origin of the weak peak in the shock compression spectrum in Fig. 1 at 1.84 eV (indicated by the arrow), attributing it to the fading C-HH transition [open diamond symbol in Fig. (2)]. From our results, we conclude that the bulk DPs of the Γ band are sufficient to predict the electronic structure of QWs at $\sigma_{LS} < 2$ GPa.

At $\sigma_{LS} > 2$ GPa, increasing deviations from the calculated trend can be observed with decreasing QW widths in Fig. 2(a). Figure 3(a) shows that this non-linear behavior precedes the abrupt loss of PL intensity, indicative of the DIT in the conduction band of uniaxially strained GaAs.[13] In the bulk material, the DIT was detected at 3.4 GPa, and this response agrees well with the calculated crossing point of the Γ_C-Γ_V and X-Γ_V shifts as shown by the black curves in Fig. 3(b). In the QWs, the Γ_C and Γ_V bands in these calculations are replaced by the quantum states C and LH, respectively, and can be treated using first-order perturbation theory.[31] It was shown that the resulting transition acquires an anticrossing character expressed as follows:[32]

$$E_{\pm}(\sigma_{LS}) = 1/2\Big((E_1 + E_2) \pm ((E_1 - E_2)^2 + 4V^2)^{1/2}\Big),$$

where E_1 and E_2 correspond to C-LH and X-LH shifts, respectively, and V is the interaction potential. To draw the curves in Fig. 3(b), we used the above equation to fit the data of the narrowest 3.4 nm QW (symbols). The plotted data were truncated below the HH-LH crossover at 1 GPa and normalized to the ambient C-LH threshold of 206 meV. The X band (fitted) is lowered in energy by the ambient difference between the C state and the Γ_C band, $\Delta E_{C\text{-}\Gamma}$, while using the same bulk volumetric and shear DPs for this band.[30] Good agreement between the band anticrossing point at 2.6 GPa and the abrupt PL intensity decay is obtained using the fitting values of $\Delta E_{C\text{-}\Gamma} = 105$ meV and $V = 15$ meV as shown by the blue curves in Fig. 3(b). It shows that the increasing deviations from the calculated trend with the decreasing QW widths in Fig. 2(a) occur due to the increasing anticrossing character between the X band and the emerging quantum states.

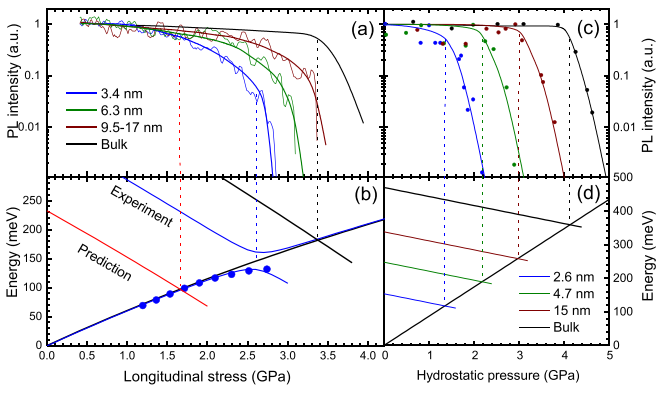

FIG. 3. (a) PL intensity changes of different QW peaks under dynamic compression. For clarity purposes, the intensity of the three widest and partially overlapping QWs is combined into a single curve. The smooth eye guiding lines are obtained by polynomial data fitting. (b) Corresponding changes in the electronic structure calculated using DPs of bulk GaAs. The same results under hydrostatic pressure (Ref. 16) (c) and their corresponding calculations (d).

The $\Delta E_{C\text{-}\Gamma}$ fit parameter value obtained is lower than the estimated result of 145 meV. This estimate was made by assuming that the contributions from the C and LH states to the ambient C-LH threshold of 206 meV are equal to the reported 0.65/0.35 alignment ratio between the conduction and valence bands of GaAs and $Al_{0.3}Ga_{0.7}As$.[33] Exciton binding energy of the order of 10 meV is added to this estimate.[30] However, the schematic electronic structure in Fig. 2 shows that the X band in the $Al_{0.3}Ga_{0.7}As$ barrier is even lower than its equivalent in GaAs. Since X bands in both materials are expected to shift down in a similar manner (red arrows), the $\Delta E_{C\text{-}\Gamma}$ estimate must be increased by an additional 90 meV[33] to account for the type-II DIT in a real space. The prediction of the real space crossover using the total value of $\Delta E_{C\text{-}\Gamma} = 235$ meV is shown by the red curve in Fig. 3(b).

It is unlikely that the large discrepancy between the prediction and the experimental observation in Fig. 3(b) originates from the uncertainties of the X band in $Al_{0.3}Ga_{0.7}As$ or the assumption of equal shifts for this band in two different materials. To examine this hypothesis, we used the same procedure in Figs. 3(c) and 3(d) to model the DIT in equivalent QWs under hydrostatic pressure. The PL intensity data in Fig. 3(c) are reproduced from Ref. 16 (symbols with eye guiding curves). The calculations in Fig. 3(d) were repeated by adding the HH-LH split in the $\Delta E_{C\text{-}\Gamma}$ estimations since the deviatoric part of the strain tensor is absent in the case of hydrostatic pressure and the HH state remains higher in energy during hydrostatic compression. Good agreement between the calculated type-II DIT thresholds and the abrupt PL changes is shown by the vertical dashed lines for all QW widths.

Hence, we conclude that the predicted type-II DIT for uniaxial strain is correct, but it is suppressed by additional interactions within the QWs. In fact, the rate of PL intensity loss in the 3.4 nm QW accelerates near the predicted 1.6 GPa threshold as shown by the vertical dashed line in Fig. 3(a). However, the change is relatively gradual, and significant PL signal is retained up to the abrupt type-I DIT at 2.6 GPa, indicating the suppression of the type-II DIT. The suppression argument also agrees with the smaller anticrossing character predicted for the real-space transitions than for the reciprocal-space transitions,[8] but theoretical calculations beyond semi-empirical approaches are needed to fully explain our findings. Finally, we note that we examined the simplest form of interactions, where the [100] uniaxial strain is aligned with the quantization axis, while much stronger perturbations are anticipated for other symmetry reduction cases.[34]

In summary, we investigated the DIT in GaAs QWs under uniaxial strain applied along the quantization axis using a unique experimental approach utilizing dynamic compression. The observed DIT was shown to deviate from the predicted real-space type-II transformation using bulk DPs. This finding emphasizes the need to examine electronic structures at the nanoscale using well-defined large anisotropic strains. In addition, it has implications for practical applications of nanostructures, suggesting that engineering of large anisotropic strains can be used to improve the

efficiency of optoelectronic devices beyond the real space DIT limits.

The dynamic compression experiments and their analysis were carried out at Washington State University and were supported by DOE/NNSA (No. DE-NA0000970). Kurt Zimmerman and Yoshi Toyoda are thanked for their help with the experiments.

The crystal growth work was carried out by Alliance for Sustainable Energy, LLC, the Manager and Operator of the National Renewable Energy Laboratory for the U.S. Department of Energy (DOE) under Contract No. DE-AC36-08GO28308. Funding for this effort was provided by the U.S. Department of Energy Office of Energy Efficiency and Renewable Energy Solar Energy Technologies Office. The views expressed in this article do not necessarily represent the views of the DOE or the U.S. Government. The U.S. Government retains and the publisher, by accepting the article for publication, acknowledges that the U.S. Government retains a nonexclusive, paid-up, irrevocable, worldwide license to publish or reproduce the published form of this work, or allow others to do so, for U.S. Government purposes.

[1]A. L. Edwards and H. G. Drickamer, Phys. Rev. **122**, 1149 (1961).
[2]G. L. Bir and G. E. Picus, *Symmetry and Strain-Induced Effects in Semiconductors*, edited by D. Louvish (Wiley, New York, 1974).
[3]E. Ertekin, P. A. Greaney, D. C. Chrzan, and T. D. Sandsb, J. Appl. Phys **97**, 114325 (2005).
[4]G. Bester, A. Zunger, X. Wu, and D. Vanderbilt, Phys. Rev. B **74**, 081305(R) (2006).
[5]A. M. Smith, A. M. Mohs, and S. Nie, Nat. Nanotechnol. **4**, 56 (2009).
[6]A. Franceschetti and A. Zunger, Phys. Rev. B **52**, 14664 (1995).
[7]H. Fu and A. Zunger, Phys. Rev. Lett. **80**, 5397 (1998).
[8]J.-W. Luo, A. Franceschetti, and A. Zunger, Phys. Rev. B **78**, 035306 (2008).
[9]A. Franceschetti and A. Zunger, Appl. Phys. Lett. **68**, 3455 (1996).
[10]L.-W. Wang, A. Franceschetti, and A. Zunger, Phys. Rev. Lett. **78**, 2819 (1997).
[11]C. Mailhiot and D. L. Smith, Phys. Rev. B **38**, 5520 (1988).
[12]A. Zunger, Phys. Status Solidi A **190**, 467 (2002).
[13]P. Grivickas, M. D. McCluskey, and Y. M. Gupta, Phys. Rev. B **80**, 073201 (2009).
[14]S. Yang, D. Prendergast, and J. B. Neaton, Nano Lett. **10**, 3156 (2010).
[15]M. Cardona, Phys. Status Solidi B **198**, 5 (1996).
[16]U. Venkateswaren, M. Chandrasekhar, H. R. Chandrasekhar, B. A. Vojak, F. A. Chambers, and J. M. Meese, Phys. Rev. B **33**, 8416 (1986).
[17]P. Lefebvre, B. Gil, and H. Mathieu, Phys. Rev. B **35**, 5630 (1987).
[18]A. Kangarlu, H. R. Chandrasekhar, M. Chandrasekhar, Y. M. Kapoor, F. A. Chambers, B. A. Vojak, and J. M. Meese, Phys. Rev. B **38**, 9790 (1988).
[19]N. Dai, D. Huang, X. Q. Liu, Y. M. Mu, W. Lu, and S. C. Shen, Phys. Rev. B **57**, 6566 (1998).
[20]C. Jagannath, E. S. Koteles, J. Lee, Y. J. Chen, B. S. Elman, and J. Y. Chi, Phys. Rev. B **34**, 7027 (1986).
[21]B. Gil, P. Lefebvre, H. Mathieu, G. Platero, M. Altarelli, T. Fukunaga, and H. Nakashima, Phys. Rev. B **38**, 1215 (1988).
[22]J. Lee, C. Jagannath, M. O. Vassell, and E. S. Koteles, Phys. Rev. B **37**, 4164 (1988).
[23]P. Etchegoin, A. Fainstein, A. A. Sirenko, B. Koopmans, B. Richards, P. V. Santos, M. Cardona, K. Totenmeyer, and K. Eberl, Phys. Rev. B **53**, 13662 (1996).
[24]P. Grivickas, M. D. McCluskey, and Y. M. Gupta, Appl. Phys. Lett. **92**, 142104 (2008).
[25]P. Grivickas, M. D. McCluskey, and Y. M. Gupta, Appl. Phys. Lett. **95**, 152108 (2009).
[26]P. Grivickas and Y. M. Gupta, Phys. Status Solidi B **250**, 683 (2013).
[27]J. Martinez-Pastor, A. Vinattieri, L. Carraresi, M. Colocci, Ph. Roussignol, and G. Weimann, Phys. Rev. B **47**, 10456 (1993).
[28]L. M. Barker and R. E. Hollenbach, J. Appl. Phys. **43**, 4669 (1972).
[29]L. M. Barker and K. W. Schuler, J. Appl. Phys. **45**, 3692 (1974).
[30]S. Adachi, *Physical Properties of III-V Semiconductor Compounds* (John Wiley & Sons Inc., USA, 1992).
[31]M. A. Gell, D. Ninno, M. Jaros, D. J. Wolford, T. F. Keuch, and J. A. Bradley, Phys. Rev. B **35**, 1196 (1987).
[32]J. H. Burnett, H. M. Cheong, W. Paul, E. S. Koteles, and B. Elman, Phys. Rev. B **47**, 1991 (1993).
[33]I. Vurgaftman, J. R. Meyer, and L. R. Ram-Mohan, J. Appl. Phys. **89**, 5815 (2001).
[34]C. Mailhiot and D. L. Smith, Phys. Rev. B **36**, 2942 (1987).